



Cycle 25 COS FUV Spectroscopic Sensitivity Monitor

Ravi Sankrit¹

¹ Space Telescope Science Institute, Baltimore, MD

16 August 2019

ABSTRACT

The Cycle 25 COS/FUV spectroscopic sensitivity monitor ran from 2017 December to 2019 April. The standard mode observations were obtained at Lifetime Position 4 (LP4), the nominal position for COS starting 2017 October 2, and the blue modes (G130M/1055 and G130M/1096) were obtained at Lifetime Position 2 (LP2). The time-dependent sensitivity (TDS) slopes were found to remain steady and range from 0% to $-3\% \text{ yr}^{-1}$. The program included two additional visits, during which the standard modes were observed at Lifetime Position (LP3) to provide a check on the TDS at the previous lifetime position. It was found that the TDS is largely independent of lifetime position. In this ISR we describe the program and its execution, and we provide a summary of the analysis and results.

Contents

1. Introduction	2
2. Program Design	2
3. Observations	4
4. Analysis and Results	4
4.1 Regular TDS Monitor	4
4.2 Lifetime Position 3 Check	7

5. Reference Files Delivered	9
6. Continuation Plan	9
Change History for COS ISR 2019-18	9
References	9
Appendix A	10

1. Introduction

The initial discovery of declines in sensitivity in several COS spectroscopic modes was reported by Osten et al. (2010). Monitoring programs were initiated to follow these trends. The Far-Ultraviolet (FUV) Time-Dependent Sensitivity (TDS) monitoring programs and their results have been described in a series of publications (Osten et al. 2011, Bostroem et al. 2015, De Rosa et al. 2016, 2017, 2018). The temporal sensitivity variations are modeled as functions of wavelength for each combination of grating (G130M, G160M, G140L) and segment (FUVA, FUVB). These are included in the TDS reference file, TDSTAB, which is used in CalCOS in association with the photometric throughput reference file, FLUXTAB, to obtain flux calibrated data.

The Cycle 25 FUV TDS monitor (PID 15384, PI R. Sankrit) consisted of two components. The first was the regular monitor, during which observations of the flux calibration standards, GD 71 and WD 0308–565, were obtained every two months between 2017 December and 2018 November. By the time the monitoring observations started, COS had been operating at LP4. The second component of the program was to check the consistency of the time-dependent sensitivity between LP4 and the previous lifetime position, LP3, and consisted of one set of observations of each target, with COS operating at LP3.

2. Program Design

The FUV TDS program is designed to obtain regular observations of flux calibration standards using the shortest and longest central wavelength standard settings of each grating, and additionally G130M/1222 (first offered to the community in Cycle 20) and the “blue modes,” G130M/1055 and G130M/1096. The two white dwarf standards, GD 71 and WD 0308–565, have been used for the FUV TDS monitor since the move to LP2 in Cycle 20. The choice of target for each cenwave and segment is based on optimizing the signal-to-noise ratio (S/N) achieved, while minimizing the impact on detector lifetime. The modes tracked in the Cycle 25 program with GD 71 and WD 0308–565 and the exposure times used are listed in Tables 1 and 2, respectively. These are unchanged from Cycle 24 with the exception of G130M/1327/FUVB, which is no longer monitored as a consequence of the COS2025 policy (Oliveira et al. 2018).

The exposure times were determined by requiring a S/N of 15 per resel at the wavelength of least sensitivity for all the standard modes, except G130M/1222. For the blue modes and for G130M/1222, the goal was to obtain $S/N \sim 25$ per resel at the

Table 1. Modes Tracked Using GD 71

Grating	Cenwave	Segment	t_{exp} (s)
G130M	1096	B	737
G160M	1577	A	104
	1623	A	155

Table 2. Modes Tracked Using WD 0308–565

Grating	Cenwave	Segment	t_{exp} (s)
G130M	1055	A	363
	1222	both	254
	1291	both	309
	1327	A	326
G160M	1577	B	342
	1623	B	416
G140L	1105	A	375
	1280	both	376

wavelength of maximum sensitivity, which ensured that $S/N > 15$ for $\lambda > 1030 \text{ \AA}$ for G130M/1096/FUVB, and for $\lambda > 1130 \text{ \AA}$ for G130M/1055/FUVA and G130M/1222. This requires one orbit per visit for GD 71 and two orbits per visit for WD 0308–565. Since there are no lamp lines available in the wavelength range covered by G130M/1096/FUVB, the GD 71 visits include a wavelength calibration lamp observation with 1096/FUVA that is obtained immediately after the science exposure, at the same Optics Select Mechanism 1 (OSM1) position.

The visit structure and sequence of observations in the Cycle 25 program follows the “complete monitoring sequence” implemented in Cycle 24 (PID 14854, PI G. De Rosa), described in De Rosa et al. (2018). Based on the analyses of the Cycle 24 data, it was determined that the “reduced monitoring sequence” (using one orbit every alternate month) was not necessary, and therefore was dropped in the Cycle 25 program.

All observations with the standard modes are obtained at the nominal (current) COS FUV lifetime position (LP4), while the blue modes are observed at LP2. At the beginning of Cycle 25, on 2017 October 2, COS FUV operations transitioned from LP3 to LP4. In order to check the behavior of the TDS at LP3, two observation sequences, one for each target, were included as part of the Cycle 25 program.

Table 3. Regular Program Observation Dates

Obs. Date	Visit No.	Target
2017-Dec-26	02	GD 71
2017-Dec-27	01	WD 0308–565
2018-Feb-20	03	WD 0308–565
2018-Feb-20	04	GD 71
2018-Apr-10	06	GD 71
2018-May-11	55	WD 0308–565
2018-Jun-07	07	WD 0308–565
2018-Aug-14	09	GD 71
2018-Oct-30	10	WD 0308–565
2018-Nov-10	11	GD 71

Table 4. LP3 Check Observation Dates

Obs. Date	Visit No.	Target
2018-Aug-27	13	GD 71
2019-Apr-16	59	WD 0308–565

3. Observations

The data used in the regular FUV TDS analysis were based on the set of observations shown in Table 3, organized by the observation date. GD 71 is not visible between the end of April and the beginning of August and therefore has only five visits. Visit 08, targeting WD 0308–565, was dropped from the final analysis since the data appeared to be compromised due to guide star acquisition.

Table 4 lists the two visits during which observations were obtained at LP3. The WD 0308–565 LP3 check was originally scheduled for 2018 August. The original observations and three subsequent repeats failed, and the data were successfully obtained only in 2019 April.

All the data from successful observations are available in the archive.

4. Analysis and Results

4.1 Regular TDS Monitor

The data were analyzed following the method described in Bostroem et al. (2015), using the script *cos_tds_analysis.py*. Calibrated `_x1d.fits` files obtained as part of

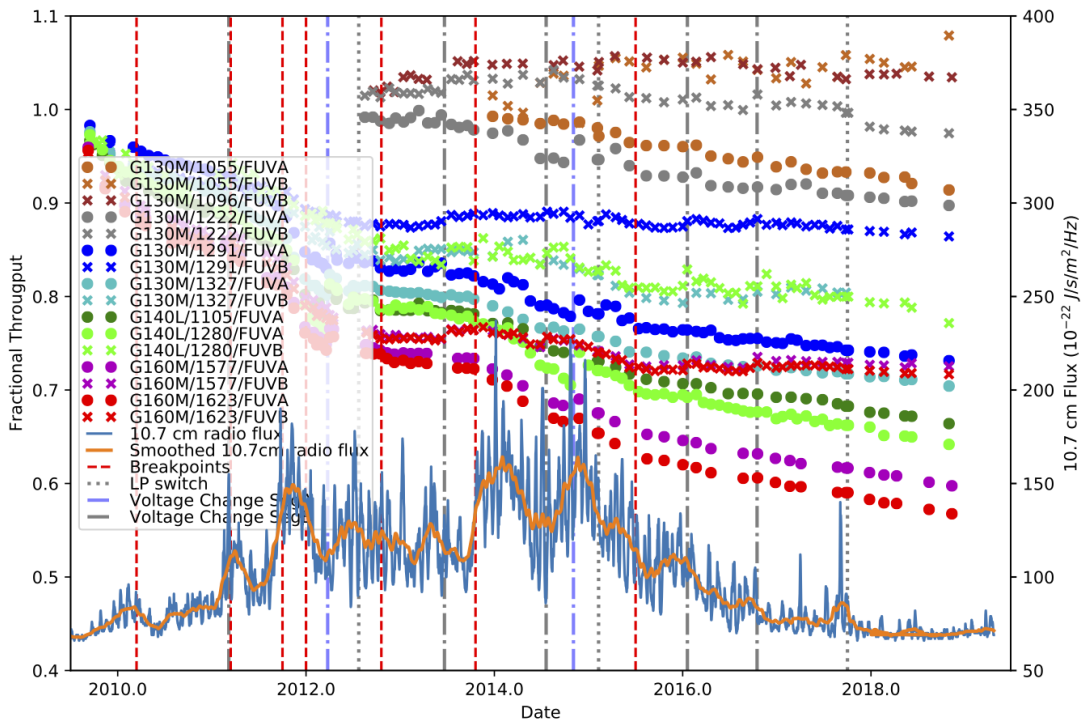


Figure 1. The change in COS FUV spectroscopic sensitivity with time. The fractional throughput relative to first light is shown for each mode tracked as a function of decimal year. The solar activity directed at Earth, as measured by the 10.7 cm flux, is shown as a solid blue line (overlaid with a smoothed version in orange). Dashed red vertical lines show the breakpoints used in the piecewise linear function that models the TDS. The dates of the LP moves are shown as dotted grey lines, and the dot-dashed lines indicate when the operational voltage was changed.

the FUV TDS monitoring programs from 2009 through 2018 November were used in the analysis. The net counts were binned over 5 \AA for the medium-resolution modes and over 20 \AA for the low-resolution modes. The data obtained at LP2, LP3, and LP4 are scaled to data obtained at LP1, LP2, and LP3, respectively, using contemporaneous observations obtained at the different LPs. The data are fit using a piecewise linear function with breakpoints at decimal years 2012.20, 2011.20, 2011.75, 2012.00, 2012.80, 2013.80, and 2015.50, the last introduced at the end of Cycle 24 (De Rosa et al. 2018). The overall relative sensitivity is normalized to 1.0 at the time of first light (2009 May 1). Figure 1 shows a summary plot of the sensitivity against time. Also plotted for comparison is the solar activity directed toward the earth as a function of time. The 10.7 cm solar fluxes are obtained periodically from the Space Weather Prediction Center of the National Oceanic and Atmospheric Administration.

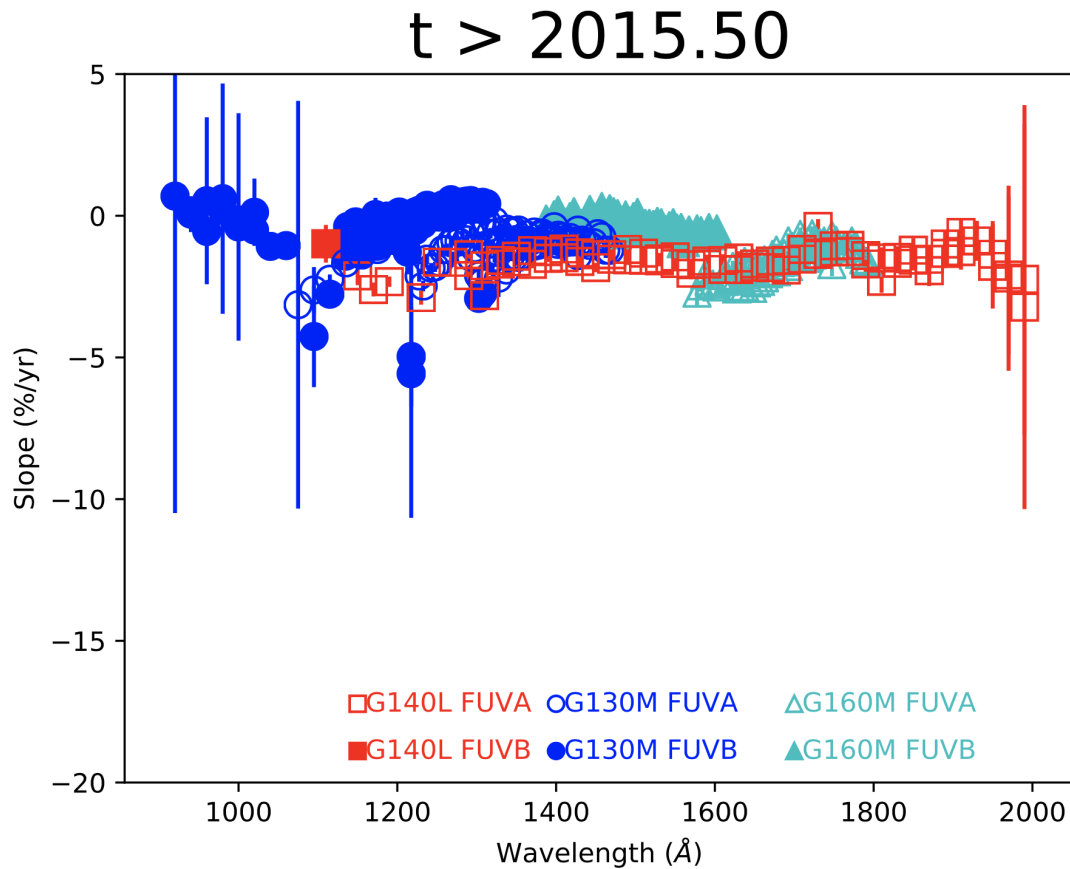


Figure 2. The COS TDS slopes obtained at the end of the regular Cycle 25 observations (2018 November) expressed in percentage change per year plotted against wavelength for the different gratings and segments. Note that the G140L FUVB slope is a for a single 20 Å bin in the cenwave 1280 setting. The errors on the derived slopes are small except in some cases near the detector edges and around airglow lines.

The TDS slopes for the linear fits since the last breakpoint (2015.5) are relatively uniform over the COS wavelength range, varying between approximately 0% and $-3\% \text{ yr}^{-1}$. In Figure 2 the TDS slopes are shown plotted against wavelength for each grating and segment.

The TDSTAB reference file was left unchanged, since the resulting absolute and relative flux accuracies are within 5% and 2%, respectively, for all the modes, except for G140L/1280/FUVB and the blue modes, for which the requirements are less stringent. The absolute flux accuracy for the blue modes (G130M/1055 and 1096) is 20%.

Table 5. Dates and Time Intervals for LP3/LP4 Comparison

Target	Lifetime Pos.	Epoch 1	Epoch 2	Δt (yr)
GD 71	LP3	2017-Sep-25	2018-Aug-27	0.921
	LP4	2017-Oct-03	2018-Aug-14	0.863
WD 0308–565	LP3	2017-Sep-25	2019-Apr-16	1.556
	LP4	2017-Oct-05	2019-Apr-16	1.529

Table 6. Exposure ROOTNAMEs Used for LP3/LP4 Comparison

Grating	Cenwave	Segment	LP3 (epoch 1)	LP3 (epoch 2)	LP4 (epoch 1)	LP4 (epoch 2)
G130M	1222	both	ldcv20elq	ldqj59jtq	ldcv22wpq	ldv005f9q
	1291	both	ldcv20enq	ldqj59jvq	ldcv22wrq	ldv005g2q
	1327	A	ldcv20epq	ldqj59jxq	ldcv22x1q	ldv005gjq
G160M	1577	B	ldcv20euq	ldqj59jzq	ldcv22wtq	ldv005gbq
	1577	A	ldcv21f8q	ldqj13e9q	ldcv23mtq	ldqj09g0q
	1623	B	ldcv20ewq	ldqj59k1q	ldcv22wvq	ldv005gdq
	1623	A	ldcv21faq	ldqj13ebq	ldcv23mvq	ldqj09g2q
G140L	1105	A	ldcv20f0q	ldqj59k5q	ldcv22wzq	ldv005ghq
	1280	both	ldcv20eyq	ldqj59k3q	ldcv22wxq	ldv005g4q

4.2 Lifetime Position 3 Check

The TDS is assumed to be independent of the LP at which observations are obtained, and hence the same TDS model is applied to observations obtained at LP3 and LP4. To check this assumption, we compared the fractional decline in the detected source count rates between two epochs for each cenwave observed at LP3 and LP4. The first epoch observations were all obtained as part of the Cycle 24 FUV TDS program (PID 14854). For the second epoch, we used the LP3 observations listed in Table 4 and the LP4 observations obtained as part of the regular FUV TDS monitor closest in time to these. In the case of GD 71, we used Visit 09 (Table 3). However, successful LP3 observations of WD 0308–565 were obtained only after the completion of the regular Cycle 25 monitor, so we used observations from Visit 05 of the Cycle 26 FUV TDS monitor (PID 15535), which were obtained on the same day as the LP3 observations. The dates of the observations and the time intervals between the epochs are listed in Table 5, and the exposures used are listed in Table 6.

For all the data used, the net count rates were obtained from the calibrated `_x1d.fits`. The fractional change in the net count rates, expressed in units of $\% \text{ yr}^{-1}$, is

$$\Delta C(t_1, t_2) = 100 \times ((C_{t_2} - C_{t_1})/C_{t_1}) \times 1/(t_2 - t_1), \quad (1)$$

where C_{t_1} and C_{t_2} are the count rates measured in the Epoch 1 and Epoch 2 data, respectively, and $t_2 - t_1$ is the time interval between the observations in years for the mode being considered (Δt column in Table 5).

If the original assumption that the TDS is independent of LP is valid, then there should be no difference in these count changes between LP3 and LP4 observations. To visualize the results, we plot the percentage change in sensitivity per year at LP3 and LP4, and the difference between these changes, against wavelength for each monitored mode. One example, for G130M/1291 segment FUVA, is shown in Figure 3, while plots for all the modes are in Appendix A.

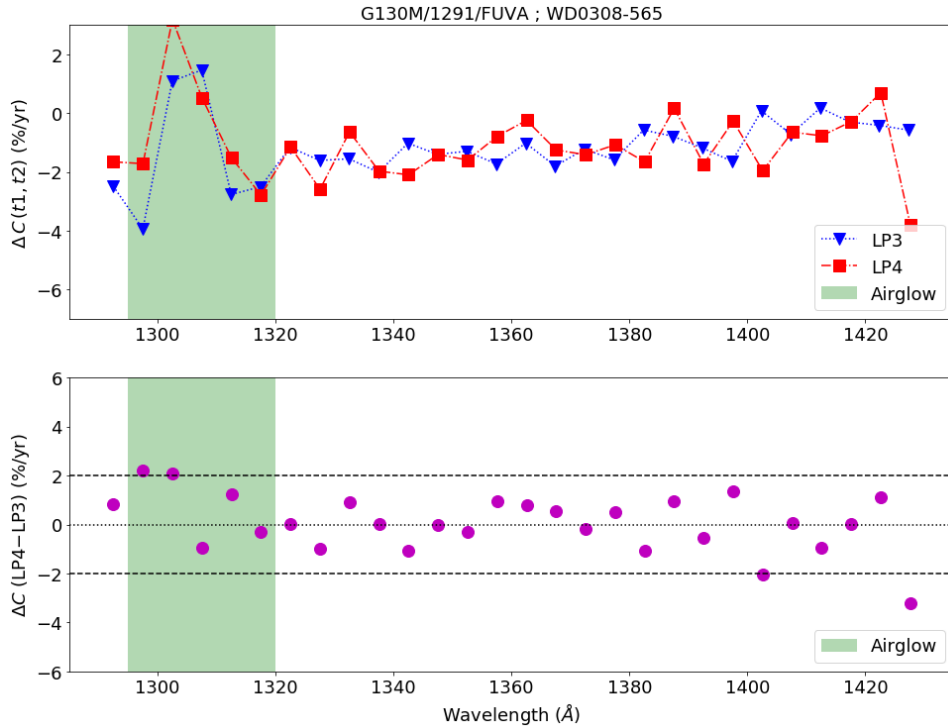


Figure 3. Results for G130M/1291, segment FUVA. Top panel: Changes in the net count rates at LP3 (blue triangles) and LP4 (red squares), expressed in $\% \text{ yr}^{-1}$, calculated over 5 \AA bins. The region shaded in green is the location of the O I airglow line. The bottom panel shows the *difference* between the LP4 and LP3 change (magenta circles), also in $\% \text{ yr}^{-1}$.

The changes in the LP3 and LP4 count rates track each other closely, and differences between the two are generally within $2\% \text{ yr}^{-1}$ for all the modes. Larger deviations may be present at the detector edges, at wavelengths contaminated by

airglow lines, and at wavelength ranges affected by gain sag at LP4. Identified gain-sag holes are shown in the plots for G130M/1222/FUVB, G160M/1577/FUVB, and G160M/1623/FUVB (Appendix A).

The only significant difference is detected in the G130M/1222 segment FUVB data at wavelengths shorter than about 1140 Å. At these wavelengths the throughput, and correspondingly the count rates, is very low. Moreover the throughput decline is very steep; therefore, small differences in the wavelength solution might result in significant differences in the binned net counts.

Since the detected differences are compatible with our tolerance, we conclude that the TDS does not depend on the Lifetime Position.

5. Reference Files Delivered

No reference files were delivered based on these analyses and results.

6. Continuation Plan

In Cycle 26, the regular monitoring of the FUV TDS continued in program 15535 (PI R. Sankrit). The targets and frequency of visits are the same as in Cycle 25. Starting with the visits in 2019 February, the new cenwaves G160M/1533 and G140L/800/FUVA were included in the sequence of observations.

Change History for COS ISR 2019-18

Version 1: 16 August 2019 – Original Document

References

Bostroem, K. A., Aloisi, A., Debes, J., et al. 2015, COS TIR 2014-05, “COS FUV Time-Dependent Sensitivity Monitoring”

De Rosa, G., Sana, H., Ely, J., & the COS team. 2016, COS ISR 2016-13, “Cycle 22 COS/FUV Spectroscopic Sensitivity Monitor”

De Rosa, G., & the COS team. 2017, COS ISR 2017-10, “Cycle 23 COS/FUV Spectroscopic Sensitivity Monitor”

De Rosa, G., & the COS team. 2018, COS ISR 2018-09, “Cycle 24 COS/FUV Spectroscopic Sensitivity Monitor”

Oliveira, C., De Rosa, G., Mackenty, J., et al. 2018, COS ISR 2018-16, “COS2025: A New Strategy to Prolong the Lifetime of the COS/FUV Detector to 2025”

Osten, R. A., Ghavamian, P., Niemi, S.-M., et al. 2010, COS ISR 2010-15, “Early Results from the COS Spectroscopic Sensitivity Monitoring Programs”

Osten, R. A., Massa, D., Bostroem, A., Aloisi, A., & Proffitt, C. 2011, COS ISR 2011-02, “Updated Results from the COS Spectroscopic Sensitivity Monitoring Program”

Appendix A

We present plots showing the change in count rate against wavelength for LP3 and LP4. For an explanation of the quantities plotted and the symbols, see the caption for Figure 3. Additionally, identified gain-sag holes at LP4 are shown as orange boxes in the plots. The LP4 declines are significantly larger in regions affected by gain sag. Note that 5 Å bins are used for all the modes except G140L/1105/FUVA and G140L/1280/FUVA, for which 20 Å bins are used.

